MECHANICS OF ADVANCED MATERIALS AND STRUCTURES

Impact of the geometry of inclusions at the micro-scale on the overall stochastic properties

H. D. Miranda, F. M. Andrade Pires, A. T. Marques

ABSTRACT

In this contribution, the establishment of relationships between the microstructure of the material and the macroscopic properties is numerically investigated. The material under study is composed by inclusions randomly distributed on a uniform matrix and its heterogeneous nature is characterized by the size, shape, spatial distribution and properties of the inclusions. To conduct these analyses, a general framework that generates and simulates representative volume elements (RVEs) based on the commercial finite element (FEM) software ABAQUS and existing homogenization techniques is developed. Two and three-dimensional RVEs are generated and the variation of the properties investigated using a statistical approach.

1 Introduction

1.1 Motivation

In the last decades, a significant number of studies on computational homogenization and micro mechanical modeling of materials have been conducted. Several important contributions have been made to the field where we highlight the pioneering work of Hill (1984) on some basic principles of homogenization, the work of Moulinec and Suquet (1998) formalizing the homogenization approach for nonlinear composites, and more recently, the work of Temizer and Wriggers (2008) proposing a contact homogenization methodology. The potential contribution of micromechanical modeling to the understanding of the physics of certain materials, the deformation mechanisms and the damage process can be extremely important. Furthermore, micromechanical modeling can also be an important design tool to tailor new materials. For example, in the case of unidirectional fiber reinforced composites, it can establish a relation between the effect of the random distribution of fibers with the effective properties. In addition, the micromechanical modeling approach combined with homogenization techniques provides a more hypothesis-free strategy to describe the macroscopic behaviour of materials than other classical methods. Since it can replicate the non deterministic nature of materials considering random generated microstructures, it is also more suitable for reliability studies. Hence, computational homogenization is a very powerful and promising tool. However, it is a complex and demanding field, because.

- It requires a statistically accurate generation of the geometry of the models, which should reproduce the true random nature of the microstructure of real materials.
- The geometrical complexity can result in extremely expensive computationally problems or difficult to mesh by automatic procedures.
- It is hard (or not possible yet) to access the precise morphology, or access the constitutive laws and properties of the materials at the microstructure. For instance, the interface transition zone (ITZ) in concrete, described by Scrivener *et al.* (2004), remains an important issue of research.

- The homogenization strategy for nonlinear regimes is still on debate by the scientific community.
- The simulation of microstructures conducts to significant amounts of data and calculation errors which are difficult to manage automatically.

The above reasons justify why a large amount of homogenization research work only deals with simple, isotropic, two phase RVEs, based on a matrix reinforced (or weakened) by disk or spherical inclusions.

1.2 Practical applications and RVE size

Practical applications impose restrictions on the morphology of the RVE due to the lack of information of the micro structural geometry or the inability to manage the complexity of the geometry. Because of these reasons, the level of detail of the micro structure, the geometrical features of the inclusions, the size of the RVE, and other simplifications should be carefully decided. In fact, there is a well known compromise between RVE size, accuracy and computational time to perform the simulations. For instance, in the case of unidirectional fibre reinforced composites (FRC), periodic considerations of simplistic RVE structures, assuming a hexagonal periodic distribution, can be successfully employed for some specific proposes, but it has been shown (see for instance Trias *et al.* (2006)) that they cannot capture important characteristics related to the distribution of the micro fields in the material (e.g. probability of failure).
The size of the RVE depends on the physical properties to homogenize. For instance, in a study of homogenization of a two-phase three dimensional Voronoi mosaic (see Kanit *et al.* (2003)), it is shown that the RVE size differs if the thermal conductivity or elastic properties are considered. Also Trias (2006) has found that for a typical unidirectional carbon fiber-reinforced composite (considering the transverse plane), the minimum RVE size is related to the chosen physical properties to consider, such as, similarities in the distributions of stress or strain in the matrix, elastic properties, average deformation energy, etc.
In the literature, some studies investigate the minimum RVE size for specific materials and applications. For instance, the work of Drugan and Willis (1996) attempts to determine the minimum RVE size associated to the effective modulus of a two phase random material composed by a dispersion of non overlapping identical spheres. The work of Trias (2006) establishes the minimum RVE size for unidirectional FRC according to the geometry and micro field criterion. Kanit *et al.* (2003) provides a good review of the methodologies proposed to define the minimum RVE size.

1.3 Fluctuations of results, RVE size and morphology

The relation between the fluctuation of results and the geometry of the RVE constituents has been addressed for some particular cases. Ostoja-Starzewski (1999) considered 2D RVEs based on a matrix with thin needle-shaped inclusions to obtain homogenized elastic properties. Considering a constant range of fluctuations on the homogenized properties it was observed that the required size of the RVE depends on the aspect ratio of the inclusions. Ren and Zheng (2004) and Ren and Zheng (2002) considered 2D RVEs based on polycristals and determined a relation between the size of the RVEs and the level of anisotropy of single crystals.

1.4 Attempts to reduce the size of the RVEs

In order to reduce the size of the RVEs required to perform homogenization, some methodologies have been proposed. Zeman and M.Sejnoha (2001) considered laboratorial images of a unidirectional FRC of graphite, and used an optimization technique to generate a small volume of the geometry. This element of volume tends to be more representative than a volume extracted from the original images with the same size at a random position. In Gusev (1997) and Kanit *et al.* (2003), effective properties have been obtained using a large amount of smaller samples (Monte Carlo method) than the representative RVE and considering the main statistics.

1.5 The morphology of the RVE and the distribution of the effective properties

The strategy to obtain the effective properties, using the Monte Carlo method with a large amount of runs, consists of estimating the expected properties of the RVE as average values obtained for a large amount of samples. The strategy is in agreement with the central limit theorem, which is valid for a large amount of samples. The central limit theorem assumes that if a random variable Y is defined as average of an amount of n random variables X_i ($1 \leq i \leq n$) with any type of distribution, then Y tends to a normal distribution as n tends to infinity, with the same expected value as X_i. However, the rate at which the variable Y approximates the normal distribution depends on the type and dispersion of the random variables X_i.
If the overall homogenized properties are considered as random variables, then the relations between the statistical distributions of those variables and the parameters of the RVE (geometry of inclusions, volume fraction, etc.) can be very important in this context. These relations can provide the roots to a more direct connection between morphology and representativeness of the RVEs. This would allow for a better understanding of the stochastic behaviour of materials, when associated with the morphology.
As the RVE size (to obtain a scatter within a given tolerance) and the geometry seem to be related in some cases, it might be possible to establish a relation between the type and parameters for the random distribution associated with the effective properties and the morphology of the RVE.

1.6 The distribution of homogenized properties and reliability of the materials

The connection between the properties of the inclusions and the variability of the homogenized material properties can be used for reliability design proposes. Furthermore, the distribution of the extreme stress and strain values at the finer scale (responsible for certain damage mechanisms), for a given set of RVEs, is probably dependent on the morphology of the components. Then, for tailored materials, it could be an interesting issue to associate the geometry of the constituents with the reliability of materials, developing for instance parametric failure, yielding, or other threshold criterion.

1.7 Outline

In this work, we start by developing a general framework that generates and simulates RVEs (in 2D and 3D). This framework is described in Section 2. The assessment and validation of the framework, which is presented in Section 3, includes the selection of an appropriate mesh refinement and the comparison of results with classical analytical models. Sections 4 to 7 report a comprehensive set of experiments on RVEs based on disc inclusions randomly distributed on a uniform matrix.
In particular, in Section 4, the type of stochastic variable that is associated with the overall homogenized elastic property of a randomly generated RVE is investigated. Section 5 illustrates how the mismatch of stiffness between matrix and inclusions can affect the spread of the homogenized properties. In Section 6, a thin interface layer that surrounds the inclusions is considered, and the influence of such interface on the overall properties is investigated. Section 7 compares the dispersion of the overall properties using models of two or three dimensions. The conclusions of the studies are summarized on Section 8.

2 Test set-up and implementation issues

In this section, the framework developed to generate RVEs of the micro structure of the material and the computation of the overall properties is described. The computational implementation within the commercial software ABAQUS is briefly explained.

2.1 Material scales and homogenization

A particular material can be often described by a model, with more or less assumptions, in accordance with the 'level' of chosen detail. For instance, a conventional steel alloy can be considered as a continuous and homogeneous material at the scale of the human eye. However, if the microscopic scale is used, the material is far from being homogeneous due to the presence of different constituents and phases. Homogenization based multi-scale models aim to describe the material behaviour at multiple scales simultaneously.
By performing the homogenization of different fields, it is possible to connect two different scales of the material. The homogenization strategy complies with certain assumptions, e.g. the energy of deformation should be the same at the two scales, in order to convert variables from one scale to the other.

2.2 RVE type and average quantities

In the literature, several shapes for the RVE have been advocated. Nevertheless, in this work, the shape of the RVE considered is either a square (in 2D) or a cube (in 3D). If the RVE is copied in a grid pattern, defined by the directions and length of the edges, it should produce a repetitive medium. For any field of variables, the average quantities of the RVE can be obtained according to Xia *et al.* (2003) using expression (1).

$$\langle \bullet \rangle \quad = \quad \frac{1}{V_\mu} \int_{\Omega_\mu} \bullet \, dV. \tag{1}$$

In expression (1), Ω_μ represents the domain of the RVE and V_μ the volume occupied by that domain.

2.3 Hill-Mandel principle, kinematic restrictions and equilibrium

As mentioned before, the conservation of deformation energy between scales is usually considered. This is also known as the Hill-Mandel principle, given by:

$$\bar{\mathbf{P}} : \dot{\bar{\mathbf{F}}} = \left\langle \mathbf{P}_\mu : \dot{\mathbf{F}}_\mu \right\rangle. \tag{2}$$

In equation (2), $\mathbf{P}$ refers to first Piolla-Kirchhoff stress tensor, $\mathbf{F}$ represents the deformation gradient, where the presence of index μ indicates lower scale quantities, while the bar indicates the upper scale quantities. On the other hand, the deformed position of a particle at position $\mathbf{Y}$ in the RVE around a point $\mathbf{X}$ can be expressed as:

$$\mathbf{y}(\mathbf{Y}, t) = \bar{\mathbf{F}}(\mathbf{X}, t)\mathbf{Y} + \tilde{\mathbf{u}}(\mathbf{Y}, t). \tag{3}$$

In equation (3), $\bar{\mathbf{F}}(\mathbf{X}, t)$ denotes the deformation gradient around the point $\mathbf{X}$ at the upper scale. Therefore $\bar{\mathbf{F}}(\mathbf{X}, t)\mathbf{Y}$ represents the homogeneous component of the deformations, and $\tilde{\mathbf{u}}(\mathbf{Y}, t)$ represents the displacement fluctuation at the finer scale.
The equilibrium conditions of the RVE, expressed in the strong form, are defined by:

$$Div_Y \mathbf{P}_\mu + \mathbf{B}_\mu = 0, \tag{4}$$

$$\mathbf{P}_\mu \mathbf{N} + \mathbf{T}_\mu = 0. \tag{5}$$

In expressions (4) and (5), Div_Y represents the divergence with respect to the reference position $\mathbf{Y}$, $\mathbf{B}_\mu$ is the body force per unit reference volume, $\mathbf{T}_\mu$ is the traction per unit reference area on the boundary surface having the normal direction $\mathbf{N}$. The equilibrium of the RVE can be expressed in the weak form using the virtual work

principle, which leads to:

$$\int_{\Omega_\mu} \mathbf{P}_\mu : \nabla_Y \boldsymbol{\eta}\, dV - \int_{\Omega_\mu} \mathbf{B}_\mu \dot{\boldsymbol{\eta}}\, dV - \int_{\partial\Omega_\mu} \mathbf{T}_\mu \dot{\boldsymbol{\eta}}\, d\mathbf{A} = 0. \tag{6}$$

In expression (6), $\boldsymbol{\eta}$ is any virtual admissible displacement field.

2.4 Periodic Boundary Conditions

In order to comply with the Hill-Mandel principle, the kinematic restrictions and the equilibrium conditions (Equations (2) to (6)), one of the classical boundary conditions can be considered:

- Taylor assumption;
- Linear displacements on the boundary;
- Periodic displacements and anti periodic tractions on the boundary;
- Uniform traction on the boundary.

The last three types of boundary conditions have an asymptotic convergence of the homogenized properties as the size of the RVE increases (Miehe (2003)). Nevertheless, the boundary condition that enforces periodic displacements is the one that is able to produce better results in the linear regime according to several studies (Terada *et al.* (2000), Miehe (2003)). Therefore, the periodic boundary condition was the one employed in the current study. This boundary condition assumes that in the boundary, the fluctuations of displacements at the finer scale $\tilde{\mathbf{u}}(\mathbf{Y}, t)$ are periodic. In a more explicit sense, the displacement on a pair of opposite boundary surfaces (with their normals along the Y_i axis) is given by expressions (7) and (8) according Xia *et al.* (2003):

$$u_i^{j+} = \bar{\varepsilon}_{ik} y_k^{j+} + \tilde{u}_i, \tag{7}$$

$$u_i^{j-} = \bar{\varepsilon}_{ik} y_k^{j-} + \tilde{u}_i. \tag{8}$$

In expression (7), the index $j+$ means along the positive Y_j direction and the index $j-$ means along the negative Y_j direction. The difference between equations (7) and (8) leads to equation (9) (Xia *et al.* (2003)).

$$u_i^{j+} - u_i^{j-} = \bar{\varepsilon}_{ik}(y_k^{j+} - y_k^{j-}) = \bar{\varepsilon}_{ik} \Delta y_k^j. \tag{9}$$

In equation (9), Δy_k^j is constant, and represents the edge length of the RVE in the direction j.

2.5 Discretization and implementation on ABAQUS

The enforcement of periodic boundary conditions on ABAQUS was implemented using linear constrains equations between the degrees of freedom. The equation constrains in ABAQUS allows to implement equation (9) directly on opposed boundary nodes. If the boundary nodes do not exactly match the opposite ones, then those nodes are related, with the nearest ones on the opposite face, through interpolation and again equation (9). Alternative strategies for the enforcement of periodic boundary conditions on non conform meshes can be found in Tyrus *et al.* (2007), Nguyen *et al.* (2012), Reis and Andrade Pires (2014).

2.6 Algorithm used to generate the RVE

In order to generate the geometry of the model, a classical general algorithm, the so-called random sequential addition (RSA)(Widom (1966)), was adopted. In this algorithm, the fist inclusion is inserted in a random position

of the matrix. Then, the next inclusions are introduced sequentially one by one in a random position such that they do not overlap the ones already placed in the RVE (this is usually achieved by trial and error approach). If there are no modifications to the original algorithm (e.g. domain decomposition), then as the number of inclusions increases, the computational time increases in a factorial order ($O(n!)$). This happens because when a new inclusion is inserted, the overlap with all other particles has to be verified. Despite the availability of more efficient algorithms (see for instance Melro *et al.* (2008) or Wongsto and Li (2005)), the RSA algorithm was selected due to its simplicity, general purpose and guarantee of generation of a perfectly random distribution by construction.
As stated in Section 2.2, the material portion with the form of a square or cubic domain, should be able to create a medium without discontinuities on the inclusions, as the RVE is placed in a orthogonal regular mesh. In order to fulfill this criterion, the RSA algorithm is slightly modified: when an inclusion is placed randomly, copies of the same inclusion are also placed attending to the periodicity of the medium and the boundary. Therefore, the verification of overlapping also has to be verified for all copied instances. The modified RSA algorithm adopted is presented in Figure 1.

2.7 Strategy used to compute the overall elastic properties

The macroscopic elastic properties are obtained from the constitutive elastic matrix, which is obtained from a set of stress strain-pairs. For a given RVE, different strain states are applied independently using the periodic boundary conditions, defined by expression (9). For each of those strains, the stress state is computed using the FEM method, and converted into homogenized stress using the average definition described in expression (1). Considering the fact that the constitutive elastic matrix and each of the stress-strain pairs, should be in agreement with relation (10), the constitutive elastic matrix can be obtained.

$$\boldsymbol{\sigma} = \mathbf{C}\,\boldsymbol{\varepsilon}. \tag{10}$$

In relation (10), $\boldsymbol{\sigma}$ is the stress tensor, $\boldsymbol{\varepsilon}$ is the strain tensor and $\mathbf{C}$ is the constitutive elastic matrix. Assuming a generic anisotropic material, the constitutive elastic matrix is given by:

$$\mathbf{C} = \begin{bmatrix} \frac{1}{E_1} & \frac{-\nu_{23}}{E_2} & -\frac{\nu_{31}}{E_3} & & & \\ -\frac{\nu_{12}}{E_1} & \frac{1}{E_2} & -\frac{\nu_{32}}{E_3} & & & \\ -\frac{\nu_{13}}{E_1} & -\frac{\nu_{23}}{E_2} & \frac{1}{E_3} & & & \\ & & & \frac{1}{2G_{23}} & & \\ & & & & \frac{1}{2G_{31}} & \\ & & & & & \frac{1}{2G_{12}} \end{bmatrix}. \tag{11}$$

In expression (11), E is the elasticity modulus, ν is the Poisson ratio and G the shear modulus. The sub-indexes stand for the direction associated with each variable. Considering the symmetry of the matrix $\frac{\nu_{23}}{E_2} = \frac{\nu_{32}}{E_3}$, $\frac{\nu_{31}}{E_3} = \frac{\nu_{13}}{E_1}$ and $\frac{\nu_{12}}{E_1} = \frac{\nu_{21}}{E_2}$. This implies that, in the 3D case, nine coefficients of the $\mathbf{C}$ matrix are not known and six on the 2D case.

2.8 Work flow of the implementation

The flowchart of the general framework, which generates RVEs and computes homogenized properties in the commercial software ABAQUS and MATLAB, is presented in Figure 2.

In the first step, MATLAB is used to run scripts that allow the generation of the geometric definition of the micro structure of the RVE. Then, MATLAB calls ABAQUS which uses a Python script to generate a working model (mesh, boundary conditions etc.), and proceeds to the FEM stress strain analysis. From the obtained stress state, the homogenized stress is computed (using a Python script) and then retrieved back to MATLAB. Finally, MATLAB is used to compute the elasticity matrix and the homogenized elastic properties of the overall RVE.

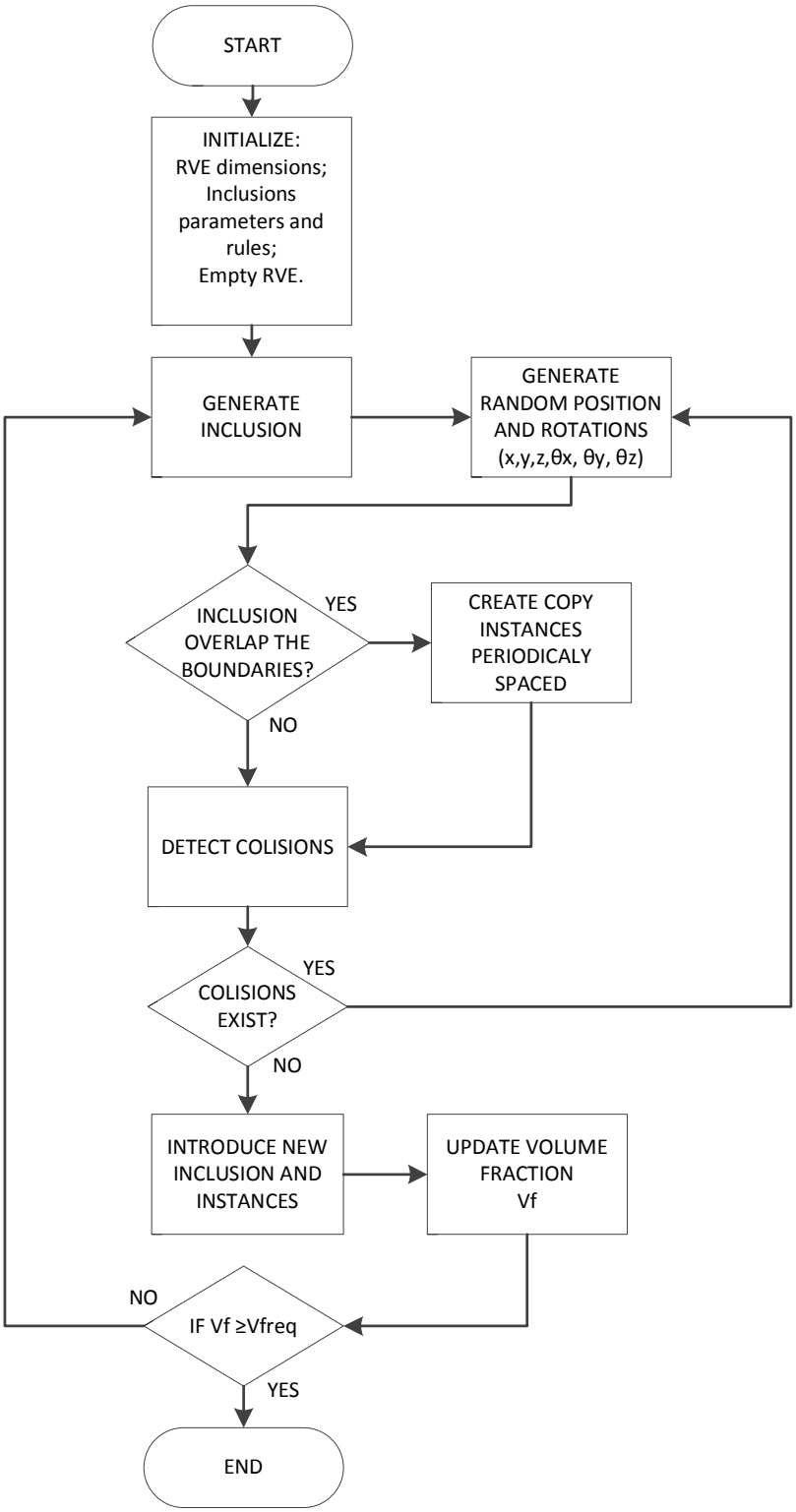

Figure 1: Flowchart of the RSA modified algorithm to generate the RVE geometry.

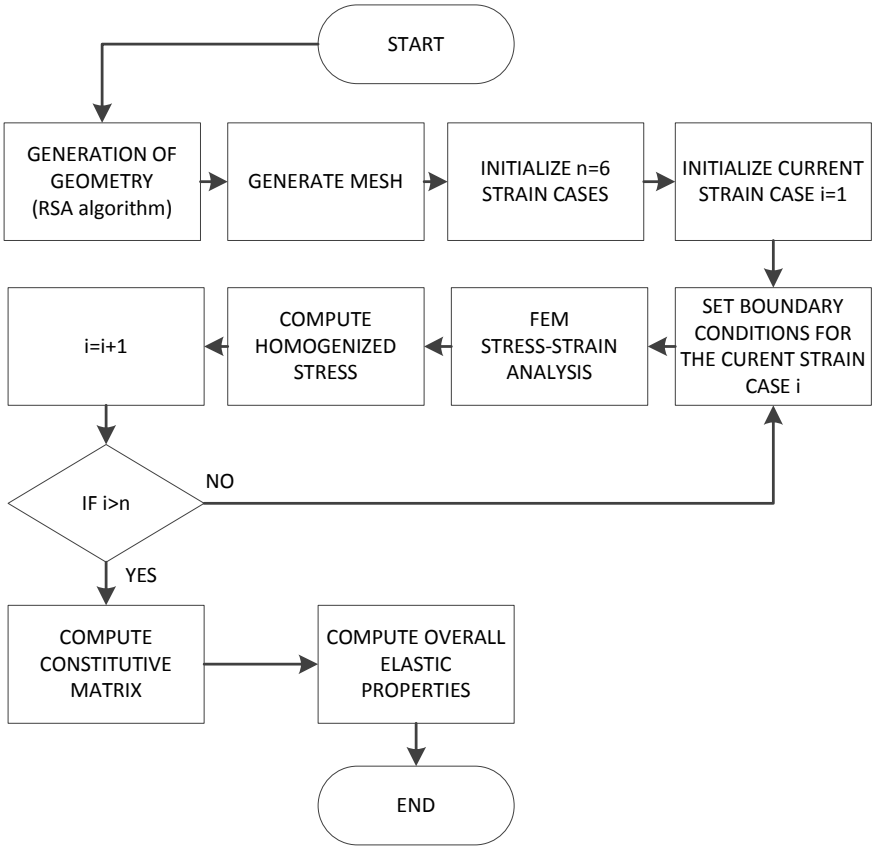

Figure 2: Flowchart of the general framework.

3 Validation of the framework

3.1 Parameters of the RVE

The materials properties (elasticity modulus and Poisson ratio) are gathered from a set of the World Wide Failure Exercise for E glass/MY750/HY917/DY063 but the volume fraction reduced, see Soden *et al.* (1998). The parameters considered for the RVE analysis, are given in Table 1. In this table, the index i stand for inclusion, the index

L/R	V_f	E_i (GPa)	ν_i	E_m (GPa)	ν_m
20	0.3	74	0.2	3.35	0.35

Table 1: Parameters of the used RVE.

m stands for matrix, L is the size of the edge of the RVE and V_f is the inclusion volume fraction. The scalar E is the elasticity modulus and ν is the Poisson ratio.

3.2 Mesh refinement

Since this example aims to evaluate the dispersion of the homogenized properties due to geometrical factors, it is very important to reduce the contribution of the calculation errors. Otherwise, the dispersion of the homogenized properties will be biased. Therefore, in order to control the precision of the results due to the refinement of

the mesh, a single geometrical definition of the RVE was used to generate models with different mesh sizes, and compute the elastic properties with different mesh sizes. Each of the meshes is discretized essentially by quadrilateral elements and a small fraction with triangular elements. The homogenized properties corresponding to each mesh and the relative error with regard to the most refined mesh are given in Tables 2 and 3.

Mesh	Mesh size	E1(GPa)	E2(GPa)	v21	v12	G(GPa)
1	1	5.3276	5.3142	0.3256	0.3265	1.9622
2	0.5	5.5128	5.5008	0.3262	0.3269	2.0390
3	0.25	5.6058	5.5893	0.3264	0.3274	2.0693
4	0.125	5.6308	5.6129	0.3268	0.3279	2.0799
5	0.0625	5.6370	5.6193	0.3269	0.3279	2.0828
6	0.03125	5.6388	5.6211	0.3268	0.3279	2.0835
7	0.015625	5.6393	5.6216	0.3268	0.3279	2.0837

Table 2: Homogenized elastic parameters for different mesh sizes.

Mesh	Mesh size	%Error E1	%Error E2	%Error v21	%Error v12	%Error G
1	1	5.5265	5.4672	0.3670	0.4295	5.8306
2	0.5	2.2432	2.1481	0.2021	0.2991	2.1446
3	0.25	0.5946	0.5740	0.1307	0.1514	0.6937
4	0.125	0.1507	0.1544	0.0101	0.0064	0.1817
5	0.0625	0.0413	0.0412	0.0037	0.0035	0.0432
6	0.03125	0.0082	0.0082	0.0004	0.0004	0.0089
7	0.015625	0.0000	0.0000	0.0000	0.0000	0.0000

Table 3: Estimated error for the elastic properties considering mesh 7 as reference.

Considering the results obtained and the compromise between calculation time and precision, the mesh selected to perform the tests of this section was Mesh 6. That mesh is depicted on Figure 3, and a detail of the mesh in Figure 4.

3.3 Analytical models and bounding limits

In order to assess the liability of the results, the Hashin-Shtrikman (see Hashin and Shtrikman (1963)) models have been used. Expression (12) considers an extreme situation, where the phases of the materials have a series arrangement, which provides a lower limit E_s for the elasticity modulus. On the other hand, expression (13) considers the other extreme situation, where the phases of the materials have a parallel arrangement, that provides a upper value E_p for the elasticity modulus.

$$E_s = \left[\frac{V_i}{E_i} + \frac{1 - V_i}{E_m}\right]^{-1}, \tag{12}$$

$$E_p = E_i V_i + E_m(1 - V_i). \tag{13}$$

In expressions (13) and (12), index i stands for the inclusions and the index m stands for matrix. The scalar V represents the volume fraction while E represents the elasticity modulus. For a better approximation, the classic Halpin-Tsai model (see Halpin and Kardos (1976)) that estimates the elastic properties has been used. According to this model, a property P can be estimated by:

$$n = \frac{\frac{P_i}{P_m} - 1}{\frac{P_i}{P_m} + \xi}, \tag{14}$$

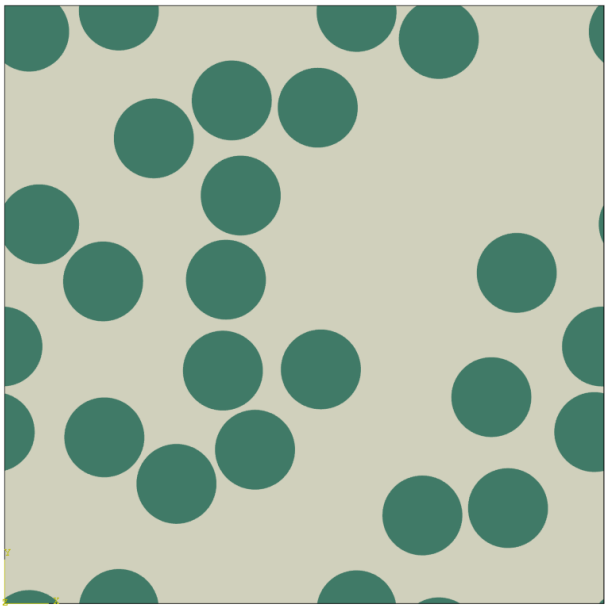

Figure 3: Periodic model used to test the influence of the mesh on the homogenization.

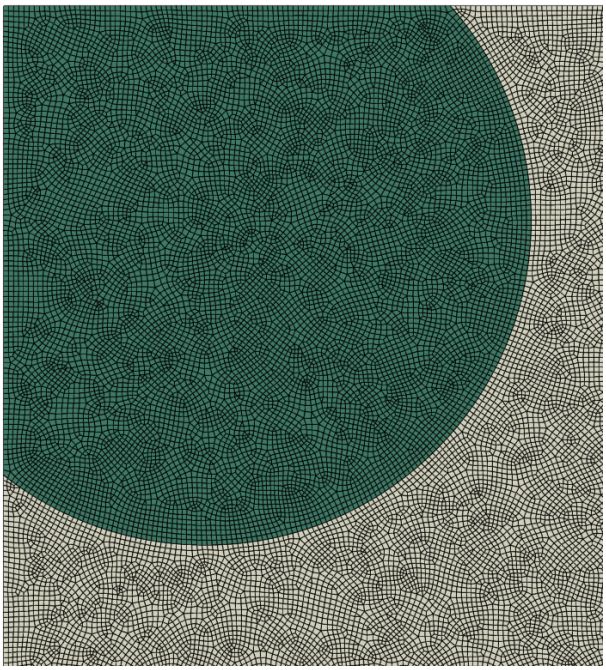

Figure 4: Detail of the mesh 6 in the model (1 060 812 elements CPS4R, 32 580 elements CPS3, 1 079 025 nodes).

$$P = P_m \frac{1 + \xi\, n\, V_i}{1 - n\, V_i}. \tag{15}$$

In expressions (14) and (15), P is an arbitrary property to estimate (e.g. elasticity modulus or Poisson ratio) and n is a temporary variable. The parameter ξ is a fitting factor, which usually takes the value of 1 if P is the elasticity modulus or 2 if P is the Poisson ratio. The results obtained, considering the specified parameters on Table 1, and using different numerical and analytical calculation techniques, are listed in Table 4.

Parameter	Value	
E (GPa)	H-S Lower limit	4.695
	H-S Upper limit	24.545
	Halpin-Tsai ξ=1	5.879
	Halpin-Tsai ξ=2	6.930
	Numerical model E_1	5.639
	Numerical model E_2	5.622
ν	Halpin-Tsai ξ=1	0.2971
	Halpin-Tsai ξ=2	0.3000
	Numerical model ν_{21}	0.3268
	Numerical model ν_{12}	0.3279

Table 4: Estimation of the parameters according to the analytical models Hashin-Shtrikman (Hashin and Shtrikman (1963)) and Halpin-Tsai (Halpin and Kardos (1976)).

4 Distribution fitting

The homogenized elastic properties of an RVE, based on disk inclusions randomly distributed, are considered as stochastic variables. Those properties are usually assumed as normal or Gaussian variables. This hypothesis will be tested in this section.
Therefore, 500 samples of RVEs with fixed parameters were generated and the homogenized properties computed, using the framework described in Section 2. The results obtained are illustrated in the histograms of Figures 5 to 9. The main statistics are presented in Table 5.

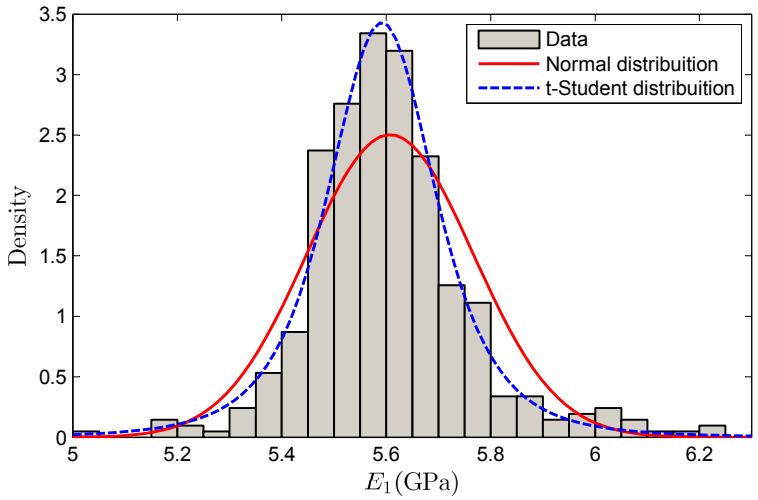

Figure 5: Homogenized elasticity modulus E_1 for 500 RVEs and fitting distributions.

In order to ensure the correct fitting of the sample results data to the distribution of the random variable, an hypothesis test was performed. The null hypothesis (H_0) considered was the following: the random variable corresponding to a given parameter is described by a certain distribution of probability (Normal and t-Student was tested), in contrast to the hypothesis that the random variable does not follow that distribution. The hypothesis test estimates the probability of obtaining such (or more extreme values) than the ones given by the sample results statistics, and considering the null hypothesis true. The χ^2 of good fitting test (see for instance Gibbons and Chakraborti (2003)) was used.
The obtained p-values presented on Table 6, correspond to the desired probability. For the Normal distribution with regard to E_1, E_2 and G p-values inferior to 5% (significance level α) were obtained wich means that the null hypothesis can be rejected safely. However, for the Poisson ratio ν_{21} and ν_{12}, the p-value obtained is higher than

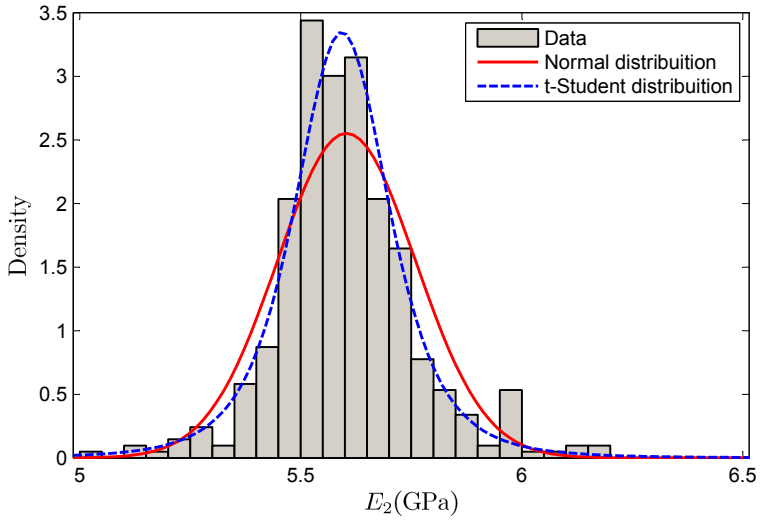

Figure 6: Homogenized elasticity modulus E_2 for 500 RVEs and fitting distributions.

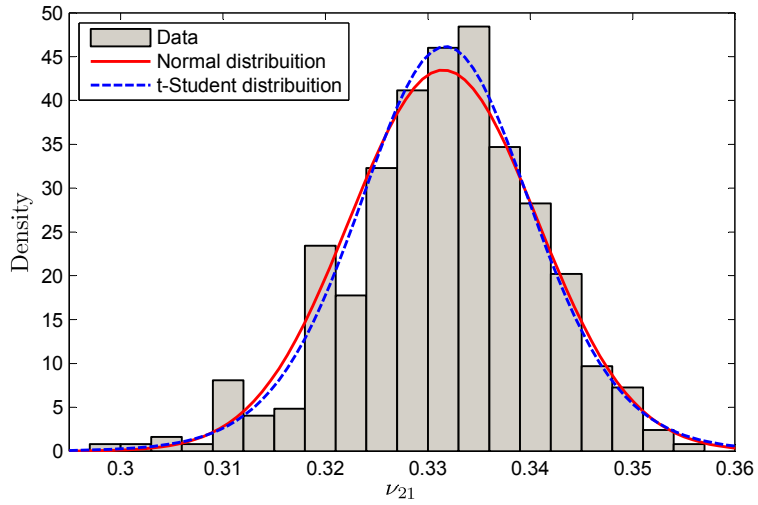

Figure 7: Homogenized Poisson ratio ν_{21} for 500 RVEs and fitting distributions.

5% which does not allow to reject the null hypothesis safely. For the t-Student distribution the p-values values are all higher than 5%, which means that the null hypothesis cannot be safely rejected, for any of the parameters.
From these results it is possible to conclude that the Normal variable is not appropriate to characterize the distribution of the homogenized Elasticity modulus and Shear modulus. Furthermore, it can be concluded that the t-Student variable can provide a reasonable approximation, better than the Normal variable.

5 Influence of the relation between the elasticity modulus of the constituents

The influence of the relation between the elasticity modulus of the constituents on the dispersion of the overall homogenized properties was studied. Four basic configuration types, for the RVE described according the data presented on the Table 7, were considered. The elasticity modulus of the matrix (E_m) is kept constant while the elasticity modulus of the inclusions (E_i) is variable. This leads to a variable ratio E_i/E_m. For each basic type of configuration, five random models are generated and then different materials properties are assigned. The results obtained for configuration 1, are summarized in Figures 10 and 11. For the other configurations, the same pattern of behaviour was observed. It can be concluded that the predictions of the numerical models are in agreement

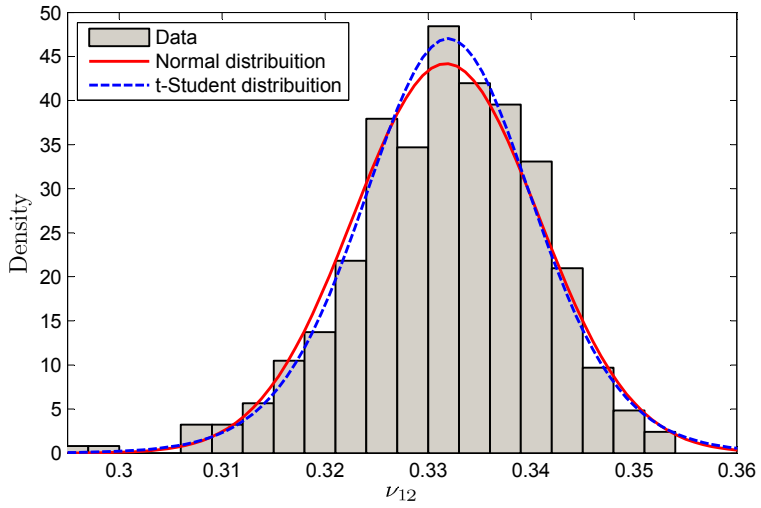

Figure 8: Homogenized Poisson ratio ν_{12} for 500 RVEs and fitting distributions.

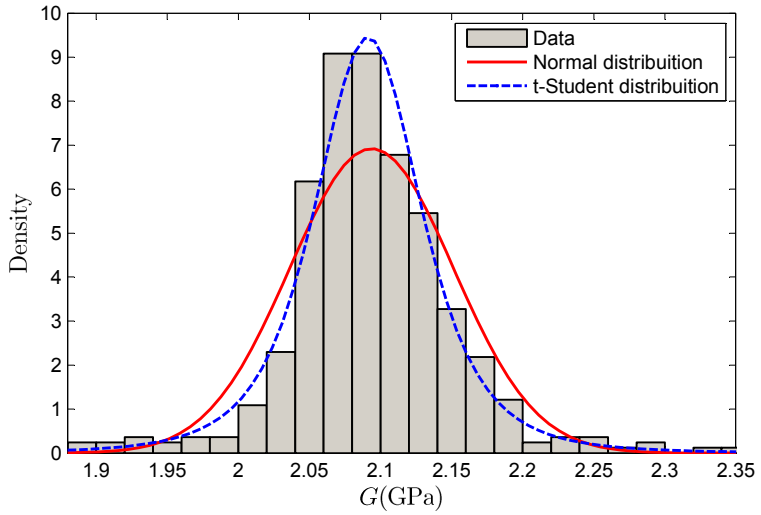

Figure 9: Homogenized shear modulus G for 500 RVEs and fitting distributions.

with the Halpin-Tsai model. Furthermore is possible to verify that for the Elasticity modulus all curves have the same shape and only intercept at the origin, forming a family. This indicates that fitting parameter ξ is strongly affected by the geometry of the RVE, but not (or very weekly) affected for the elasticity of the constituents. In this way, the Halpin-Tsai model can be used to estimate the dispersion of the homogenized elastic properties when the elasticity modulus of the constituents changes.

6 Influence of a thin interface surrounding the inclusions

Many materials have (at a fine scale) a thin interface layer surrounding the inclusions. This happens with concrete aggregates where a thin layer forms around the aggregates, which is called interface transition zone (ITZ), and is composed by an heterogeneous phase of small particles of cement. In order to provide insight on how this interface layer can affect the overall elastic properties, a study with different layer thicknesses and stiffnesses was performed. The objective was to encompass a wide set of possibilities, in order to obtain general conclusions about that effect, and do not rely on a specific material. Realistic properties have been assumed for the matrix and volume fractions according to Table 8. In Figure 12, the geometry of one of the models with disk inclusions surrounded

Parameter	mean	standard dev.	coef.var.
E1(GPa)	5.603	0.1582	2.82%
E2(GPa)	5.599	0.1555	2.78%
v21	0.3318	0.0092	2.79%
v12	0.3320	0.0090	2.70%
G(Gpa)	2.094	0.0571	2.72%

Table 5: Main statistics for the homogenized parameter on a sample size N=500.

variable	*p-value* $H_0 : Normal\ distribuition$	*p-value* $H_0 : t\ distribuition$
E_1	0.00%	7.66%
E_2	0.00%	5.69%
ν_{21}	14.93%	15.57%
ν_{12}	12.84%	10.52%
G	0.00%	15.93%

Table 6: *p-value* obtained for the χ^2 test of good fitting.

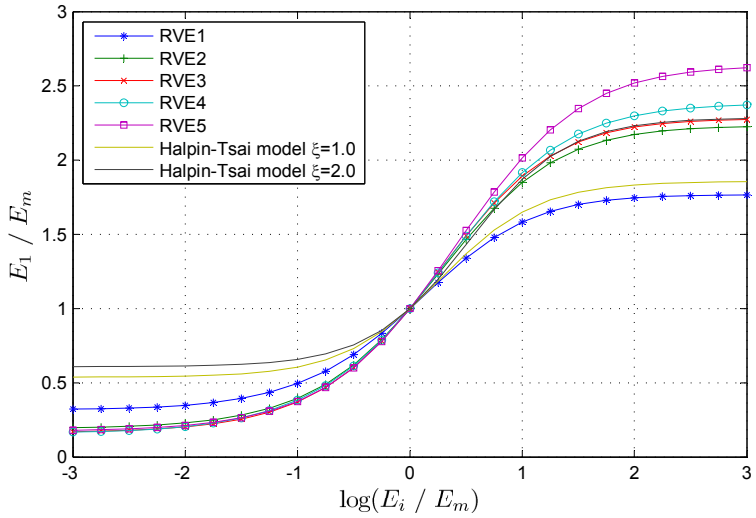

Figure 10: Evolution of the homogenized elastic modulus E_1 with the ratio E_i / E_m for the base configuration 1 and analytical Halpin-Tsai predictions.

by a thin interface layer and a detail of it are represented.

The parameters: ratio between elasticity of the overall RVE and matrix E_1/E_m, ratio between thickness of the interface and radius of inclusions t/R and the decimal logarithm between elasticity on the interface and on the

Configuration	*L/R*	V_f	E_i (GPa)	ν_i	E_m (GPa)	ν_m
1	20	0.3	varies	0.2	10	0.2
2	20	0.3	varies	0.3	10	0.3
3	20	0.2	varies	0.2	10	0.2
4	20	0.2	varies	0.3	10	0.3

Table 7: Parameters of the used RVE, for the different configurations tested.

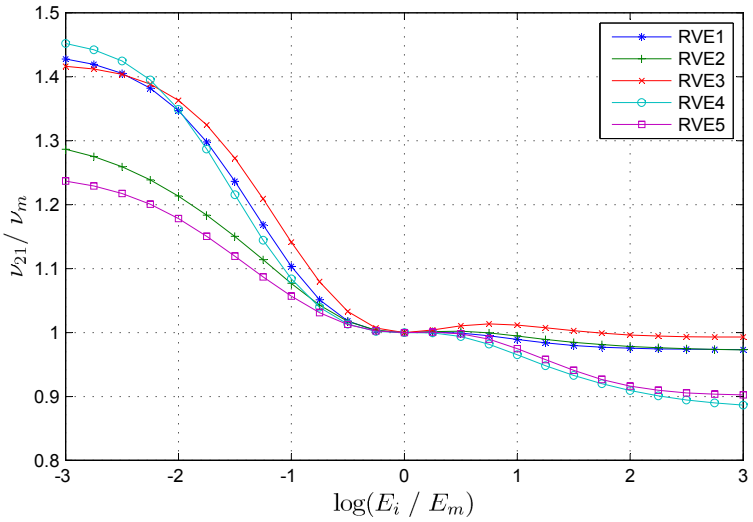

Figure 11: Evolution of the Homogenized Poisson ratio ν_{21} with the ratio E_i / E_m for the base configuration 1.

L/R	V_f	E_m(Gpa)	ν_m	E_i(Gpa)	ν_i	E_l	ν_l
20	0.4	3.35	0.35	74	0.2	varies	0.2

Table 8: RVE properties considered for test the influence of the thin layer.

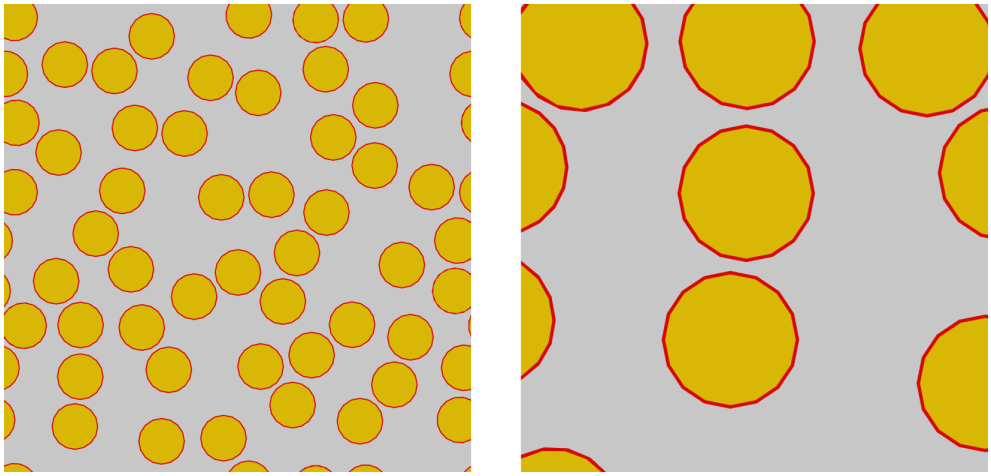

Figure 12: Geometric model of the RVE (left) and detail of the disk inclusions surrounded by a thin interface layer (right).

matrix $log(E_l/E_m)$ have been used. These dimensionless variables have been chosen in order to characterize the effect of the interface on the overall stiffness in a general manner, i.e. independently of the material. In Figure 13, the results obtained due to uniform variations of t/R and $log(E_l/E_m)$ use the same random distribution of inclusions. The plot on Figure 13 shows that the relation between variables is nonlinear. It can also be observed that the rate of variation increases with the reduction of the thickness and interface stiffness.
It can be concluded that the relation between the overall homogenized Elastic modulus and the parameters of the interface (i.e. elasticity and thickness) is highly nonlinear and very sensible to both parameters, especially for lower values of thickness and stiffness. This can be an important factor to consider when preforming simplifications on this type of RVE, e.g. use a different thickness of the interface layer to replace the real one.

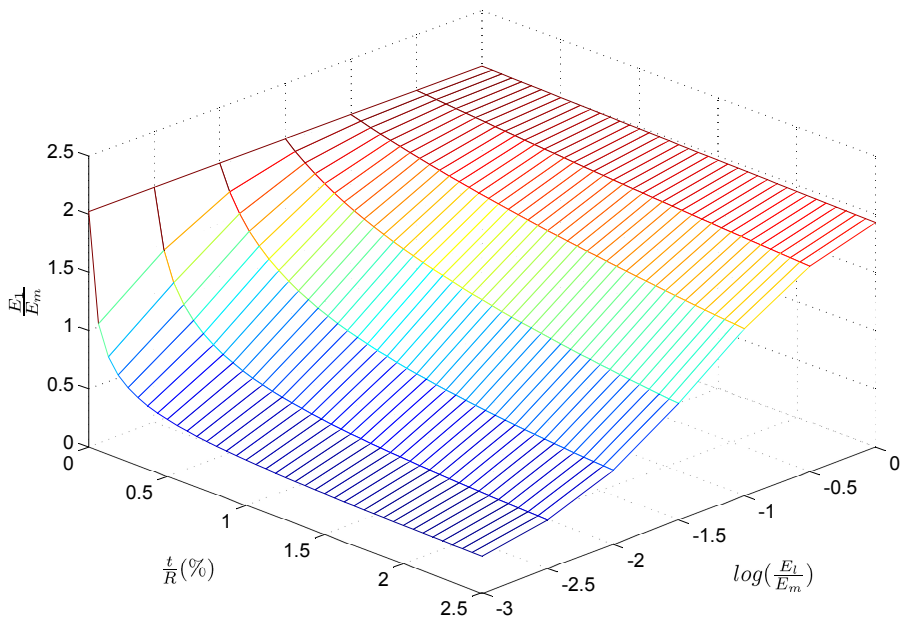

Figure 13: Influence of the thickness and stiffness of the layer on the overall stiffness of the homogenized material.

7 Numerical Experiments on Three Dimensions

In order to compare the distribution of the homogenized elastic properties between two dimensional models and three dimensional models, 50 RVE for each dimension under analysis have been generated. The properties considered for all the RVE models are described in Table 9. The plots of Figures 14 and 15 show the von Mises stress

L/R	V_f	E_i (GPa)	ν_i	E_m (GPa)	ν_m
15	0.2	74	0.2	3.35	0.35

Table 9: Parameters of the RVE.

field obtained for a 2D and 3D FEM models, respectively. As can be concluded from Table 10 and Figures 16 and 17, the dispersion of results tends to be higher in 2D than in 3D models. This can be concluded based on the coefficient of variation.

2D				3D			
Parameter	Mean	standard dev.	coef.var.	Parameter	Mean	standard dev.	coef.var.
E_1(Gpa)	4.5162	0.0455	1.01%	E_1(Gpa)	5.1216	0.0182	0.36%
ν_{21}	0.3417	0.0048	1.39%	ν_{21}	0.3235	0.0014	0.43%

Table 10: Main statistics of the homogenized elastic properties for 50 RVE in 3D and 2D.

8 Conclusions

A general framework that is able to generate 2D and 3D FEM models of arbitrary RVEs and compute homogenized elastic properties has been developed. In that framework, the geometry of the models is generated using a RSA algorithm. To perform homogenization, the classical periodic boundary condition has been employed. The implementation of the framework was done with the commercial softwares ABAQUS and MATLAB, using

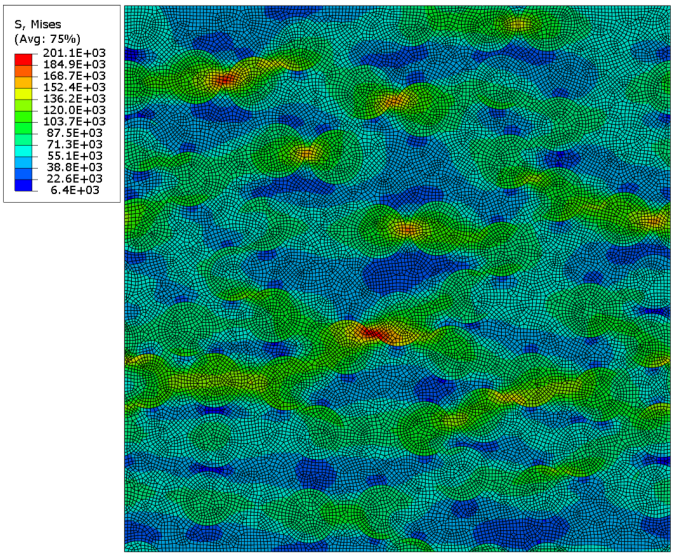

Figure 14: von Mises stress field obtained for a 2D FEM model.

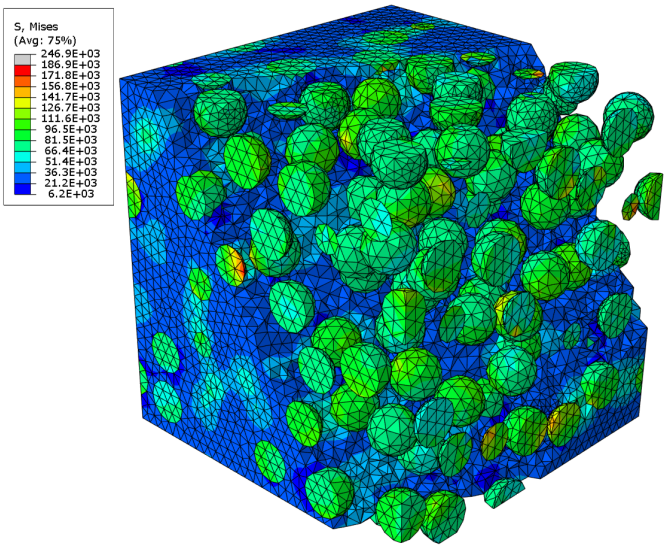

Figure 15: von Mises stress field obtained on a 3D FEM model.

Python and MATLAB scripting languages. The overall homogenized elasticity modulus and Poisson ratio, of a randomly generated 2D RVE based on disk inclusions, was computed using the numerical framework and two classical analytical models: the Hashim-Shtrikman limits and the Halpin-Tsai equations. The results obtained with the analytical models successfully validated the results obtained with the framework developed.

A total of 500 RVEs under plane strain have been generated and the overall elastic properties computed. The generated RVEs are composed by a set of disk inclusions randomly distributed on a uniform matrix. Considering the obtained data and using an hypothesis test, it can be concluded that, the homogenized elastic modulus and shear modulus distributions, do not result from a Normal random variable. It was also concluded that for the obtained distributions, a t-Student random variable could be more appropriate than the Normal variable.

The influence of the relation between the elasticity modulus of the materials on the overall homogenized elastic properties random variables was analysed. The possibility of establishing relationships between those variables and the classical analytical model Halpin-Tsai was analysed. Four types of RVE (plane strain, homogeneous matrix with disk inclusions) have been considered and for each of those types, five different RVEs have been generated.

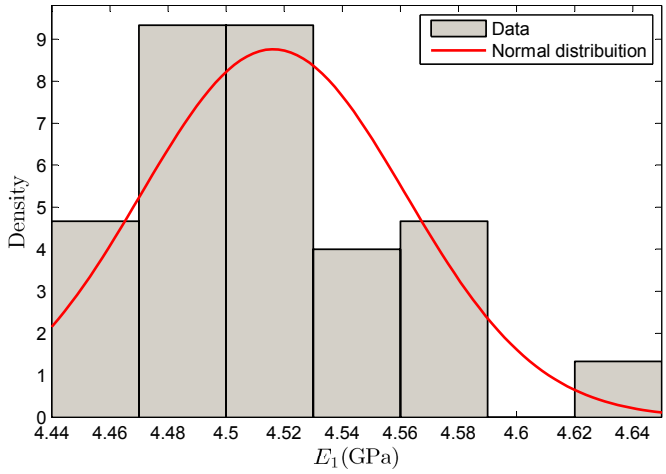

Figure 16: Histogram for the homogenized Elastic modulus considering 30 RVEs in 2D.

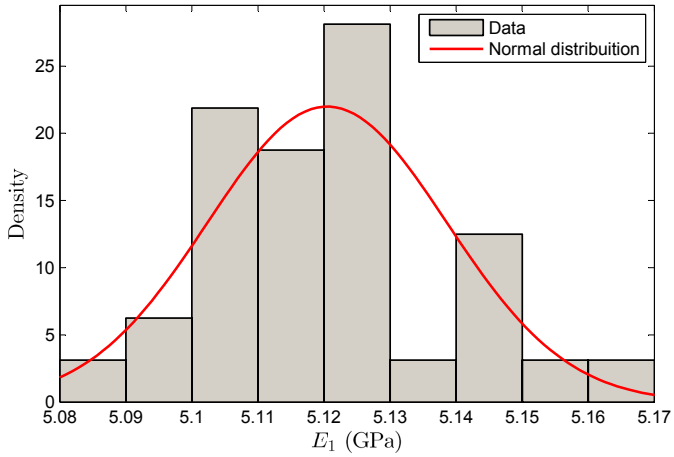

Figure 17: Histogram for the homogenized Elastic modulus considering 30 RVEs in 3D.

For each RVE, the ratio between the elasticity modulus of the matrix and the inclusions was changed according several different values and the homogenized properties computed. The obtained data shows that the dispersion of the results increases as the ratio between the elasticity modulus differs from 1. Additionally, it can be concluded that for each RVE geometry, the homogenized properties can be fairly predicted using the Halpin-Tsai model. It can also be concluded that the accurate fitting parameter ξ of that model is essentially influenced by the geometry of the RVE and almost insensitive to the ratio between the elasticity modulus of the constituents. Therefore, the Halpin-Tsai model can provide a reasonable approximation to the spreading of the homogenized elastic properties when the ratio between the elasticity modulus of the constituents changes.

The sensibility of the values obtained, for the RVE overall elastic properties, to variations on the interface layer that surrounds the inclusions was investigated. To this end, the same distribution of inclusions was adopted, and variations on the stiffness and thickness have been performed on the interface layer, and homogenized elastic properties computed. The results obtained show that the influence of those parameters is nonlinear and there is a very high sensibility of the overall elastic modulus for low values of thickness and stiffness, which can be an important factor to consider to estimate the dispersion of the results of a specific type and size of RVE. It is also important to consider this high sensibility when performing simplifications on this type of models at the interface, e.g. use different thickness for the interface layer to replace the real one.

In order to compare the distributions of the homogenized elastic properties for two and three dimensions, a total of 30 RVEs on 2D(plane strain) and 3D with same volume fraction have been generated and analyzed using the

framework described in this paper. It was possible to conclude that the Normal distribution does not have a good fitting with the results. The dispersion obtained for the 2D models was higher than the one obtained for 3D models.

References

Drugan, W. and Willis, J., 1996. A micromechanics-based nonlocal constitutive equation and estimates of representative volume element size for elastic composites. *Journal of the Mechanics and Physics of Solids*, 44 (4), 497 – 524.

Gibbons, J.D. and Chakraborti, S., 2003. *Nonparametric statistical inference*. Vol. 168. CRC press.

Gusev, A.A., 1997. Representative volume element size for elastic composites: A numerical study. *Journal of the Mechanics and Physics of Solids*, 45 (9), 1449 – 1459.

Halpin, J. and Kardos, J., 1976. The Halpin-Tsai equations: a review. *Polymer Engineering & Science*, 16 (5), 344–352.

Hashin, Z. and Shtrikman, S., 1963. A variational approach to the theory of the elastic behaviour of multiphase materials. *Journal of the Mechanics and Physics of Solids*, 11 (2), 127–140.

Hill, R., 1984. On macroscopic effects of heterogeneity in elastoplastic media at finite strain. *Mathematical Proceedings of the Cambridge Philosophical Society*, 95, 481–494.

Kanit, T., *et al.*, 2003. Determination of the size of the representative volume element for random composites: statistical and numerical approach. *International Journal of Solids and Structures*, 40 (1314), 3647 – 3679.

Melro, A., Camanho, P., and Pinho, S., 2008. Generation of random distribution of fibres in long-fibre reinforced composites. *Composites Science and Technology*, 68 (9), 2092–2102.

Miehe, C., 2003. Computational micro-to-macro transitions for discretized micro-structures of heterogeneous materials at finite strains based on the minimization of averaged incremental energy. *Computer Methods in Applied Mechanics and Engineering*, 192 (5), 559–591.

Moulinec, H. and Suquet, P., 1998. A numerical method for computing the overall response of nonlinear composites with complex microstructure. *Computer Methods in Applied Mechanics and Engineering*, 157 (12), 69 – 94.

Nguyen, V.D., *et al.*, 2012. Imposing periodic boundary condition on arbitrary meshes by polynomial interpolation. *Computational Materials Science*, 55, 390–406.

Ostoja-Starzewski, M., 1999. Scale effects in materials with random distributions of needles and cracks. *Mechanics of Materials*, 31 (12), 883 – 893.

Reis, F. and Andrade Pires, F., 2014. A mortar based approach for the enforcement of periodic boundary conditions on arbitrarily generated meshes. *Computer Methods in Applied Mechanics and Engineering*, 274, 168–191.

Ren, Z.Y. and Zheng, Q.S., 2002. A Quantitative study of minimum sizes of representative volume elements of cubic polycrystalsnumerical experiments. *Journal of the Mechanics and Physics of Solids*, 50 (4), 881 – 893.

Ren, Z.Y. and Zheng, Q.S., 2004. Effects of grain sizes, shapes, and distribution on minimum sizes of representative volume elements of cubic polycrystals. *Mechanics of Materials*, 36 (12), 1217 – 1229.

Scrivener, K., Crumbie, A., and Laugesen, P., 2004. The Interfacial Transition Zone (ITZ) Between Cement Paste and Aggregate in Concrete. *Interface Science*, 12 (4), 411–421.

Soden, P., Hinton, M., and Kaddour, A., 1998. Lamina properties, lay-up configurations and loading conditions for a range of fibre-reinforced composite laminates. *Composites Science and Technology*, 58 (7), 1011–1022.

Temizer, I. and Wriggers, P., 2008. A multiscale contact homogenization technique for the modeling of third bodies in the contact interface. *Computer Methods in Applied Mechanics and Engineering*, 198 (34), 377 – 396.

Terada, K., *et al.*, 2000. Simulation of the multi-scale convergence in computational homogenization approaches. *International Journal of Solids and Structures*, 37 (16), 2285 – 2311.

Trias, D., 2006. Determination of the critical size of a statistical representative volume element (SRVE) for carbon reinforced polymers. *Acta Materialia*, 54 (13), 3471 – 3484.

Trias, D., *et al.*, 2006. Random models versus periodic models for fibre reinforced composites. *Computational Materials Science*, 38 (2), 316 – 324.

Tyrus, J., Gosz, M., and DeSantiago, E., 2007. A local finite element implementation for imposing periodic boundary conditions on composite micromechanical models. *International journal of solids and structures*, 44 (9), 2972–2989.

Widom, B., 1966. Random sequential addition of hard spheres to a volume. *The Journal of Chemical Physics*, 44, 3888.

Wongsto, A. and Li, S., 2005. Micromechanical FE analysis of UD fibre-reinforced composites with fibres distributed at random over the transverse cross-section. *Composites Part A: Applied Science and Manufacturing*, 36 (9), 1246–1266.

Xia, Z., Zhang, Y., and Ellyin, F., 2003. A unified periodical boundary conditions for representative volume elements of composites and applications. *International Journal of Solids and Structures*, 40 (8), 1907–1921.

Zeman, J. and M.Sejnoha, 2001. Numerical evaluation of effective elastic properties of graphite fiber tow impregnated by polymer matrix. *Journal of the Mechanics and Physics of Solids*, 49 (1), 69 – 90.

Address:
Faculdade de Engenharia da Universidade do Porto
Rua Dr. Roberto Frias, s/n 4200-465 Porto
PORTUGAL
email: `dem09021@fe.up.pt`